

# Targeted Inhibition of STAT3 in Neural Stem Cells Promotes Neuronal Differentiation and Functional Recovery in Rats with Spinal Cord Injury

**Tingting Li**

Sun Yat-sen University First Affiliated Hospital

**xiaoyang zhao**

Sun Yat-sen University First Affiliated Hospital

**Jing Duan**

Sun Yat-sen University First Affiliated Hospital

**Shangbin Cui**

Sun Yat-sen University First Affiliated Hospital

**Kai Zhu**

Sun Yat-sen University First Affiliated Hospital

**Yong Wan**

Sun Yat-sen University First Affiliated Hospital

**Shaoyu Liu**

Sun Yat-sen University First Affiliated Hospital

**Zhiming Peng**

Sun Yat-sen University First Affiliated Hospital

**Le Wang** (✉ [wanglehk@163.com](mailto:wanglehk@163.com))

---

## Research article

**Keywords:** STAT3, spinal cord injury, neural stem cells, neuronal differentiation

**Posted Date:** March 17th, 2020

**DOI:** <https://doi.org/10.21203/rs.3.rs-17529/v1>

**License:** © ⓘ This work is licensed under a Creative Commons Attribution 4.0 International License.

[Read Full License](#)

---

# Abstract

## Background

Signal transducer and activator of transcription protein 3 (STAT3) is expressed in neural stem cells (NSCs), and some studies have shown that STAT3 is involved in regulating NSC differentiation. However, the possible molecular mechanism and the role of STAT3 in spinal cord injury (SCI) are unknown. Thus, in the present study, we identified possible molecular mechanisms by which STAT3 regulates NSC differentiation *in vitro* and investigated the potential therapeutic effect of transplanting STAT3-silenced NSCs in rat SCI models *in vivo*.

## Methods

*In vitro*, NSCs were divided into the following three groups: control, control shRNA, and STAT3-shRNA lentivirus groups. NSCs in each treatment group were examined for neuronal differentiation via immunofluorescence, and Western blot analysis was used to investigate the possible molecular mechanisms. *In vivo*, the rats were divided into four groups that underwent laminectomy and complete spinal cord transection accompanied by transplantation of control-shRNA-treated or STAT3-shRNA-treated NSCs at the injured site. Spinal cord-evoked potentials and the Basso-Beattie-Bresnahan score were used to examine functional recovery after SCI. Axonal regeneration and tissue repair were assessed via retrograde tracing using Fluorogold, hematoxylin-eosin staining and immunofluorescence.

## Results

Knockdown of STAT3 promoted neuronal differentiation in NSCs and mechanistic target of mammal rapamycin (mTOR) activation *in vitro*, and transplantation of STAT3-RNAi-treated NSCs enhanced rat functional recovery and tissue repair, as well as neuronal differentiation of the transplanted NSCs *in vivo*.

## Conclusions

We have provided *in vitro* and *in vivo* evidence that STAT3 is a negative regulator of NSC neuronal differentiation. Transplantation of STAT3-inhibited NSCs appears to be a promising potential strategy for enhancing the benefit of NSC-mediated regenerative cell therapy for SCI.

## Background

Spinal cord injury (SCI) often causes persistent functional deficits due to the absence of spontaneous axon regeneration and the formation of large cavities and glial scars that interrupt the ascending and descending pathways. In rodent models of SCI, levels of proinflammatory interleukins, such as interleukin (IL)-6, peak acutely in the injured areas and lead to activation of the Janus kinase 1 (JAK1)-signal transducer and activator of transcription protein 3 (STAT3) signaling pathway [1]. STAT3 signaling is also upregulated in certain neurodegenerative diseases. For instance, spinal cord microglia, reactive astrocytes and motor neuron nuclei of amyotrophic lateral sclerosis (ALS) patients showed increased levels of

phosphorylated STAT3 [2]. Another report showed that STAT3 is an important signaling component in reactive astrogliosis through the Notch1–STAT3–endothelin receptor type B (ETBR) signaling axis [3]. A growing body of literature suggests that STAT3 is an injury-induced signaling mechanism critical for various aspects of nerve regeneration [4, 5]. Moreover, *in vitro* suppression of STAT3 [6] or its conditional deletion *in vivo* [7] induces neurogenesis and inhibits astrogliosis. Thus, STAT3 appears to be the key to enhancing neurogenesis after SCI.

Neural stem cell (NSC) transplantation has been demonstrated to be a promising treatment method to improve tissue repair and functional recovery in SCI [8]. Mechanistically, NSCs might differentiate into neurons and glial cells to bridge the damaged area, re-establish the conduction pathway, and form functional synapses by expressing axonal regeneration-related genes and secreting neurotrophic growth factors in the injured spinal cord [9]. However, accumulating evidence has confirmed that NSC-based therapy cannot achieve optimal results due to the limited differentiation of neurons and the excessive differentiation of astrocytes, which contributes to glial scarring [10]. Rajalaxmi Natarajan demonstrated that an inhibitor of STAT3 promoted NSC differentiation into neurons and suppressed glial differentiation *in vitro*. However, few studies have assessed whether STAT3-silenced NSC transplantation could improve functional outcomes *in vivo*.

In this study, we first explored the effects of STAT3 RNA interference (RNAi) on NSC survival and differentiation *in vitro* and the potential mechanisms underlying these effects. Then, we injected STAT3-silenced NSCs into the injury site of a rat SCI model to investigate the effects on neurodegeneration *in vivo*. Our findings indicate that the targeted inhibition of STAT3 may represent a promising strategy to promote the neuronal differentiation of NSCs and that inhibiting STAT3 may enhance the benefit of NSC-mediated regenerative cell therapy for SCI.

## Methods

### Lentiviral vector construction

Green fluorescent protein (GFP) was carried by the lentiviral vector with a sequence that specifically silenced the STAT3 gene was constructed by GeneChem (Shanghai, China). The oligonucleotides were ligated to Hu6-MCS-Ubiquitin-IRES-puromycin (GeneChem, Shanghai, China) and have the following sequence: 5'-CAGCAGATGCTGGAACAGCAT-3'. A nontargeted sequence which have the following sequence: 5'-TTCTCCGAACGTGTCACGT-3' was carried by a control lentiviral vector. The lentivirus (LV) particles were generated as described previously [11] with a final titer of  $1 \times 10^8$  TU/mL.

### NSC isolation and culture

NSCs were extracted from the brains of the fetuses of rats on the 14th, from pregnant Sprague-Dawley (SD) rats (Laboratory Animal Center of Sun Yat-sen University, Guangzhou, China) as previously described[12]. In short, the brain tissue is mechanically cut and removed in Hanks' balanced salt solution, and the cell suspension was centrifuged at 1,000 rpm for 5 min. The supernatant was discarded and

diluting cell pellet into a single-cell suspension. NSCs were plated on a T25 culture flask (Corning, Acton, MA) containing Dulbecco's modified Eagle's medium/F-12 nutrient mixture, 1% l-glutamine (Gibco, Grand Island, NY, USA), 2% B27, 1% penicillin/streptomycin, 20 ng/mL fibroblast growth factor-2 (FGF-2) and 20 ng/mL epidermal growth factor (EGF) (Peprotech, Rocky Hill, NJ). NSCs were cultured in 5% CO<sub>2</sub> at 37 °C and passaged by weekly by digesting with Accutase (Millipore, Bedford, MA) in the medium mentioned above. 2nd to 4th passage NSCs were used in the following experiments in this study .

### NSC transfection

For cell transfection, 2nd passage neurospheres were dissociated into a single-cell suspension at a density of  $1 \times 10^5$  cells/ml and plated on coverslips coated with 0.01% poly-L-lysine (Sigma, Germany) in 12 multiwell plates (Corning, NY, USA). The cells were then kept restored in the culture medium and divided into three groups : the control group (CL), control RNAi group (LV-CL), and STAT3 RNAi (LV-STAT3) group, each group received different treatments the next day: control culture, control RNAi LV, and STAT3 RNAi LV respectively. The medium was then changed to fresh medium after 24 h. After 72 h of transfection, GFP expression was visualized by fluorescence microscopy (Carl Zeiss Axio Observer Z1). To quantify the suppress effects of RNAi on STAT3 gene, STAT3 expression in each group was examined by real-time PCR (RT-PCR) and Western blot analysis.

### Western blot

Protein lysates were extracted from the cells (N=5 per group, harvested at 3 d after transfection). Bicinchoninic acid assay (Beyotime Biotechnology) was used to measure the protein concentration and the protein was equilibrated before loading. Protein samples in each group were separated by SDS-PAGE (10% Bis-Tris gel), transferred to a PVDF membrane (Millipore, Bedford, USA) and blocked with 5% BSA (Sigma, Germany) for 1 h, followed by incubation with primary antibodies at 4 °C overnight. Primary antibodies targeting STAT3 (Abcam, USA), phosphorylated STAT3 (p-STAT3, CST, USA), mTOR (CST, USA), phosphorylated mTOR (p-mTOR, CST, USA) and glyceraldehyde-3-phosphate dehydrogenase (GAPDH; CST, USA) were used at 1:1,000 dilution. After washing the membranes in TBST (Tris-HCl buffer containing 0.2% Tween 20, pH 7.5) twice, the membranes were incubated with a filtered and peroxidase-conjugated secondary antibody for 1 h at room temperature and then washed three times in TBST. Finally, the results were observed by enhanced chemiluminescence (ECL) development system (Millibo, USA).

### RNA extraction and RT-PCR

Total cells RNA (N=5 per group, harvested at 3 d after transfection) were extracted using TRI reagent (Molecular Research Center, Cincinnati, OH). RNA was reverse transcribed into cDNA by using a reverse transcription system (Promega, Madison, WI). Real-time PCR was performed on an ABI 7900 PCR detection system (Applied Biosystems, Foster City, CA) using SYBR Green PCR Master Mix (Applied Biosystems). Parallel amplification of the GAPDH housekeeping gene was used to normalize gene expression. PCR primer sequences are listed below: STAT3 forward primer:



AATATAGCCGATTCCTGCAAGAG, reverse primer: TGGCTTCTCAAGATACCTGCTC. GAPDH forward primer: TGACGCTGGGGCTGG CATTG, reverse primer: GGCTGGTGGTCCAGGGGTCT. The relative expression level of target mRNA was calculated using the  $\Delta\Delta C_t$  method.

### Surgical procedures and cell transplantation

All experimental animal procedures have been approved by the Care and Use Committee of Sun Yat-sen University (ethics number: SYXX2012-0081) and performed in accordance with the Guide to the Care and Use of Experimental Animals provided by the National Research Council (1996, USA). All the animals were housed three to a cage with free access to food/water and kept under standardized atmosphere (temperature: 22°C, humidity: 55%, 12/12 h cycle).

Spinal cord surgery was performed on 60 adult female SD rats (200–250 g) which were bought from Sun Yat-sen University. All the rats were healthy and without previous procedures. The rats were randomly divided into four groups, including the sham group (spinal cord exposure only, n=10), the SCI group (n=15), the STAT3-shRNA-treated NSC group (LS group, n=20) and the control-shRNA-treated NSC group (LC group, n=15). In the SHAM group, rats were undergone surgery but without transection of the spinal cord; In the SCI group, rats were undergone surgery with complete transection of the spinal cord; in the LC group, rats were undergone surgery with complete transection of the spinal cord and then NSCs with transfected with control lentiviral vectors were injected into at a depth of 1 mm rostral and caudal to the injured site using a microsyringe; in the LS group, rats were undergone surgery with complete transection of the spinal cord and then NSCs with transfected with STAT3 lentiviral vectors were injected as mentioned above. As previously described[13], briefly, animals were anesthetized with 1% pentobarbital sodium (40-45 mg/kg) by intraperitoneal injection. Laminectomy was performed at the level of the 10th thoracic vertebra (T10). Next, the spinal cord was cut twice by using scissors (once caudal to T10 and once rostral to T10) for complete transection, then a 2-mm block of the spinal cord was removed. After hemostasis, the rats were injected with 5  $\mu$ L of cells (control-shRNA-treated or STAT3-shRNA-treated NSCs at a density of  $1 \times 10^5$  cells/ $\mu$ L) at a depth of 1 mm rostral and caudal to the injured site by using a microsyringe at a rate of 0.5  $\mu$ L/min. Finally, 5–0 sutures were used to suture the muscle and skin and daily intraperitoneally injected 1 mL of saline containing  $1 \times 10^5$  units of penicillin for 1 week to prevent infection and dehydration. Postsurgical care of SCI rats included manual bladder expression twice a day until bladder function was restored. Surgery was performed in a blinded manner. After 8 weeks of surgery, rats were euthanized by anesthesia with 1% pentobarbital sodium (40-45 mg/kg) and then sacrificed by CO<sub>2</sub> asphyxiation, and the spinal cord was collected at -80 °C or for perfusion.

### Basso-Beattie-Bresnahan test

The Basso, Beattie, Bresnahan (BBB) locomotor rating scale is considered a reliable tool for evaluating impairment and recovery of motor abilities in hindlimbs after spinal cord injury [14]. A total score of 21 points indicates that locomotor ability is not affected. Rats were placed in an open experimental field and allowed to move freely for 5 min, and the crawling ability was assessed by the BBB scale. Hindlimb

motor behavior was evaluated weekly for 8 weeks, with tests carried out the same time each day and grading performed by two investigators blinded to grouping.

### Spinal cord-evoked potential (SCEP) recording

At 8 weeks post injury, 20 rats (n = 5 in each group) were anesthetized with 1% pentobarbital sodium (40-45 mg/kg) and stereotaxically fixed. Then, the T5-L1 vertebrae were completely exposed. Summarily, a stimulation electrode was inserted into the T5-T6 interspinous ligaments, after that a pair of needle electrodes was inserted into the interspinous ligaments of T12-L1 for SCEP recording. The electrodes were connected to a BL-410E Data Acquisition Analysis System for Life Science (Chengdu, China). The parameters of the SCEP signals were set as follows: gain of 2,000, time constant of 0.01 s, and filtering at 300 Hz. To elicit an SCEP, a single-pulse stimulation (50 ms in duration at a frequency of 5.1 Hz and a voltage increase of 1 mV) was transmitted through the electrodes until a mild twitch of the vertebral body of the animal was observed. To obtain high-quality waveforms for the SCEP signals, we had averaged 100 SCEP responses per rat.

### Perfusion and cryosection

Eight weeks after spinal cord surgery, rats were submitted to anesthesia with 1% pentobarbital sodium (40-45 mg/kg) and sacrificed by CO<sub>2</sub> asphyxiation. Rats were then perfused transcardially with 0.9% normal saline and 400 mL 4% paraformaldehyde (PFA). T8-L1 segments of the spinal cord were postfixated with 4% PFA overnight and transferred to 30% sucrose for cryoprotection for 2-3 d at 4 °C after collection. Then, embedded tissues were sliced transversely or longitudinally at a thickness of 10 µm, mounted on polylysine-coated glass slides, and stored at -20 °C preparing for next experiments.

### Histopathological analyses

To assess the cavity area of the spinal cord, we sacrificed rats (N =5 per group) for hematoxylin-eosin (H&E) staining at 8 weeks after SCI. T8-T11 longitudinal spinal cord sections from each group were stained with H&E following standard protocols and observed in a bright field. The cavity area of these images was evaluated using NIH ImageJ software (Wayne Rasband, National Institutes of Health, Bethesda, MD). For neuron examination, transverse sections of the tissue surrounding the injured site were submitted to Nissl staining (Beyotime, Shanghai, China, C0117).

### Fluorescent immunohistochemistry

Tissue sections from rats or cells (N=5 per group) were fixed in 4% PFA for 30 min and permeabilized with 0.3% Triton X-100 for 30 min. Blocking was performed with 5% normal goat serum for 1 h, and tissue sections were incubated with primary antibodies targeting the following proteins at 4 °C overnight: β3-tubulin (1:200, CST,USA), GFAP (1:300, CST,USA), and microtubule-associated protein 2 (MAP2; 1:200, CST,USA). ProLong Gold antifade reagent containing 4'-6-diamidino-2-phenylindole (DAPI) (Thermo Fisher,USA) was used for nuclear staining. Then, the total area of target marker-positive cells was

evaluated in each visual field under fluorescence (Carl Zeiss Axio Observer Z1, Germany) with ImageJ software. Five random fields in each section and five sections per group were examined independently by 2 observers blinded to grouping.

### Retrograde axonal tract tracing

Animals (N = 5 per group) were submitted for neurons retrograde tracing by Fluorogold (FG, 1:25, Santa Cruz, CA, sc-358883) at 7 weeks after SCI. Briefly, a dorsal laminectomy was performed at T12, and 0.5  $\mu$ l of FG was injected into the spinal cord by using a microsyringe. At 1 week after injection, the animals were perfused, and the T8 segment of the spinal cord was collected to detect FG-labeled neurons.[15].

### Statistical Analysis

All statistical analyses were performed using GraphPad Prism 6 software (GraphPad Software, La Jolla, CA). All data in the study were first used Shapiro-Wilk test to evaluate normality. All data were then expressed as the mean  $\pm$  SD and were analyzed via one-way analysis of variance followed by Bonferroni post hoc tests for multiple comparisons or Student t test for pairwise comparisons.  $P < 0.05$  indicated statistical significance.

## Results

### Knockdown of STAT3 promoted neuronal differentiation in NSCs

NSCs were passaged and allowed to grow for an additional 3–5 d to form a 100- $\mu$ m-diameter neurosphere from single cells. Immunostaining of the neurospheres showed that nestin, a surface marker of neural stem and precursor cells, was strongly expressed in the neurosphere (Fig. 1A). To achieve specific knockdown of the STAT3 gene in NSCs, we transfected NSCs with shRNA-expressing LV. GFP expression was observed by fluorescence microscopy 72 h after LV infection. Western blot analysis showed that STAT3 levels were significantly lower in the LV-STAT3 group than in the LV-CL group (Fig. 1B, C). This result was also confirmed by quantitative RT-PCR analysis (Fig. 1D). Immunofluorescent staining analysis showed that targeted inhibition of STAT3 induced more NSCs to differentiate into neurons because the neuronal marker  $\beta$ 3-tubulin was expressed more frequently in the LV-STAT3 group than in the CL and LV-CL groups. However, GFAP, a specific marker of astrocytes, was expressed at markedly lower levels in the LV-STAT3 group than in the other two groups (Fig. 1E-G). These results show that we achieved specific knockdown of STAT3 gene expression in NSCs and confirm the hypothesis that targeted inhibition of STAT3 promotes neuronal differentiation of NSCs, consistent with previous research [1].

### Targeted inhibition of STAT3 promoted mTOR activation

mTOR signaling is crucial for the maintenance and differentiation of NSC development, and activation of mTOR promotes the involvement of NSCs in neurogenesis [16]. To explore the relationship between the mTOR signaling pathway and STAT3 signaling pathway in NSC differentiation, we inhibited the STAT3

signaling pathway by treating NSCs with shRNA-expressing LV. NSCs were cultured in differentiation medium after 24 h of transfection. On day 7, we performed Western blotting to examine the expression of STAT3 and mTOR. As expected, the expression of STAT3 and its activated form (p-STAT3) was significantly lower in the LV-STAT3 group than in the other two groups. Interestingly, although total mTOR expression showed no difference among the three groups, the expression of the activated form of mTOR (p-mTOR) was significantly higher in the LV-STAT3 group than in the CL and LV-CL groups (Fig. 2A, B). These results show that STAT3 inhibition activates the mTOR signaling pathway, which may promote neuronal differentiation of NSCs.

### Transplantation of STAT3-RNAi-treated NSCs enhanced functional recovery after SCI

To investigate whether transplantation of STAT3-inhibiting NSCs promotes recovery of motor function after SCI in rats, we divided the rats into 4 groups (as described in the methods section). At the 8th week, we performed hindlimb weight-bearing experiments on the 4 groups of rats. The rats in the sham group were able to use the hindlimbs to walk normally, while the rats in the LC group and the SCI group had poor hindlimb strength during walking. In contrast, rats in the LS group could sometimes stand on their hind legs to support their weight and walk slowly (Fig. 3A). In addition, the BBB functional score curve also showed that the score of the LS group was significantly higher than that of the SCI and LC groups from the 5th week to the 8th week after SCI (Fig. 3B). We also explored the electrophysiological restoration of SCEP responses. Here, SCEP waveforms of the SCI group and the LC group were significantly different from the normal SCEP waveform of the sham group, exhibiting a significantly prolonged latency and decreased amplitude. However, compared with the LC and SCI groups, the LS group had a significantly shorter SCEP latency and significantly greater amplitude (Fig. 3C-E). Taken together, these results indicate that transplantation of STAT3-inhibiting NSCs promoted functional and neurologic recovery in rats after SCI.

### Transplantation of STAT3-RNAi-treated NSCs enhanced tissue repair after SCI

To further clarify whether transplantation of STAT3-inhibiting NSCs promotes the regeneration of damaged tissues and nerves after SCI, we used H&E staining to investigate the degree of tissue repair in each group. The size of the lesion cavity was calculated in H&E-stained sections at 8 weeks post injury to detect tissue repair. In the sagittal plane, compared with the SCI and LC groups, the LS group exhibited a significantly smaller lesion area ( $P < 0.05$ ) (Fig. 4A, B). To further observe the survival of neurons around the SCI area, we performed Nissl staining on the spinal cord tissue of each group. At 3 mm from the center of the SCI area, we found extensive loss of neurons in the SCI and LC groups. In contrast, the LS group had significantly more neurons than the SCI and LC groups (Fig. 4A, C). To explore the interconnection of nerves in the injured area, we performed a retrograde tracking experiment with FG. Here, the LS group had more neurons labeled by FG than the SCI and LC groups ( $P < 0.05$ ) (Fig. 4A, D). Furthermore, at the T7 spinal cord segment, FG-labeled neurons were more frequently observed in the LS group than in the LC and SCI groups, indicating that the LS group had more nerve connections on both ends of the lesion site (Fig. 4A, D).

## Targeted inhibition of STAT3 enhanced neuronal differentiation of transplanted NSCs in spinal cord lesions

At 8 weeks after transplantation, we analyzed the differentiation of the grafted cells in the lesion site via immunofluorescence. In the LC group, the majority of GFP-positive cells expressed the astrocytic marker GFAP, and only a small number of GFP-positive cells expressed the neuronal markers  $\beta$ III-tubulin and MAP2 (Fig. 5, A, B). However, in the LS group, the percentage of GFP/ $\beta$ III-tubulin double-positive and GFP/MAP2 double-positive cells was approximately two-fold higher than that in the LC and SCI groups, whereas the percentage of GFP/GFAP double-positive cells was less than half of that in the LC and SCI groups (Fig. 5, A, B).

## Discussion

This work shows that 1) inhibiting STAT3 not only promotes NSC differentiation into neurons but also inhibits differentiation into astrocytes, potentially through mTOR activation. 2) Transplantation of STAT3-RNAi-treated NSCs into SCI rats improves functional recovery, promotes axonal regeneration and inhibits astrocyte differentiation after SCI .

After SCI, the limited regenerative capacity of the adult mammalian spinal cord has been attributed to the formation of cavities and glial scars that interrupt the ascending and descending pathways [17–19]. Now, NSC transplantation is considered an appropriate choice for treating SCI [20]. However, in contrast to NSCs in the brain, most NSCs in the spinal cord differentiate into astrocytes, and no neurogenesis has been observed after SCI [21]. STAT3 is a member of the JAK-STAT signaling family that transduces signals for many cytokines, and growth factors, including IL-6, ciliary neurotrophic factor (CNTF), leukemia inhibitory factor (LIF), EGF, and transforming growth factor  $\alpha$  (TGF $\alpha$ ), have been implicated as triggers of reactive astrogliosis [22]. STAT3 is active after SCI and plays a vital role in the differentiation of astrocytes, which contributes to glial scar formation [19, 23]. STAT3 inhibitors have been shown to reverse the inhibitory effect of STAT3 on neuronal recovery [24]. STAT3 is also expressed in NSCs, and the binding of STAT3 to the GFAP promoter is essential for astrocyte differentiation [25, 26]. Blocking STAT3 increases motor neurons and decreases GFAP-positive astrocyte differentiation of NSCs in vitro [27]. In this study, we first inhibited STAT3 expression in NSCs, which led to more neuronal differentiation. This result is consistent with previous reports and once again demonstrates that inhibiting the expression of STAT3 promotes the differentiation of NSCs into neurons while simultaneously inhibiting their differentiation into astrocytes. Interestingly, we observed that more mTOR was activated when STAT3 expression was suppressed. mTOR is a serine/threonine kinase of the phosphoinositide 3-kinase (PI3K)-related kinases and plays a relevant role in the control of the homeostasis of different compartments containing stem cells, including NSCs [28]. Some studies have reported that activation of the JAK/PI3K/Akt/mTOR signaling pathway promotes neuronal differentiation of NSCs [29]. JAK/STAT3 is another pathway parallel to JAK/PI3K/AKT/mTOR, and these two pathways competitively combine to accept JAK signals; therefore, inhibition of the JAK/STAT3 pathway may lead to more mTOR activation

and NSC differentiation to neurons. However, whether the effect of STAT3 on NSCs actually correlates with the mTOR signaling pathway requires further investigation.

We transplanted STAT3-RNAi-treated NSCs into rats subjected to SCI to evaluate whether STAT3-RNAi-treated NSCs promote functional recovery after SCI in vivo. The BBB scoring method was used to quantify motor function of the hindlimbs in this SCI animal model. A previous study showed that transplanting NSCs to rats with SCI resulted in marked improvements in mobility in 65% of the treated animals [30]. In our study, we found a more significant increase in the BBB scores of rats transplanted with STAT3-RNAi-treated NSCs, with an approximately 50% increase in BBB scores compared to the scores in the LC group at 5 weeks after SCI. Additionally, rats transplanted with STAT3-RNAi-treated NSCs tended to have higher SCEP amplitudes than rats in the LC and SCI groups, indicating that motor and sensory axonal conduction was reinforced after transplantation with STAT3-RNAi-treated NSCs [31]. H&E staining also confirmed that transplanting STAT3-RNAi-treated NSCs significantly reduced the lesion volume, potentially contributing to functional recovery after SCI [32]. More importantly, neonatal neuronal structure may enhance functional recovery after SCI through axonal regeneration, which could bridge the lesion cavity after SCI. However, according to previous studies, the microenvironments in the spinal cord lesion site after SCI lead exogenous NSCs to differentiate into astrocytes, leading to the formation of glial scars in the lesion site that are widely regarded to inhibit axon regeneration and functional recovery in the chronic phase of SCI [12, 33, 34]. In our study, compared with control-RNAi-treated NSCs, STAT3-RNAi-treated NSCs were more likely to differentiate into neurons and exhibited more dendrite outgrowth. Moreover, according to our study, neurons in the SCI area of the LS group formed more connections with the upstream and downstream neurons of the SCI area (demonstrated by more FG-labeled neurons). These connections are one of the conditions that promote better functional recovery after SCI [35]. Furthermore, less astrocytic differentiation was observed in STAT3-RNAi-treated NSCs, suggesting that the STAT3-RNAi-treated NSCs produced highly developed neurons that played an indispensable role in neurogenesis, consistent with previous studies [27]. However, these results indicated a potential better recovery after transplanting STAT3-RNAi-treated NSCs for SCI rats, but the specific mechanisms for these phenomenon are still need further investigation and it's also need more relative experiments to further confirm and clarify these findings before it could translate to other species.

## Conclusion

In summary, we have provided in vivo and in vitro evidence that STAT3 is a negative regulator of the neuronal differentiation of NSCs. The transplantation of STAT3-inhibited NSCs appears to be a promising potential strategy for enhancing the benefit of NSC-mediated regenerative cell therapy for SCI, and the discovery of a prominent role of STAT3 in NSC biology is an invaluable step forward to understanding NSC differentiation.

## Abbreviations

SCI

Spinal cord injury  
STAT3  
Signal transducer and activator of transcription protein 3  
NSC  
Neural stem cell  
shRNA  
Short hairpin RNA  
mTOR  
mammalian target of rapamycin  
IL-6  
Interleukin-6  
JAK-1  
Janus kinase 1  
ALS  
Amyotrophic lateral sclerosis  
SCEP  
Spinal cord-evoked potential  
PFA  
Paraformaldehyde  
FG  
Fluorogold  
GFAP  
Glial fibrillary acidic protein  
GAPDH  
Glyceraldehyde-3-phosphate dehydrogenase

## **Declarations**

### **Ethics approval and consent to participate**

All experimental animal procedures were approved by the Care and Use Committee of Sun Yat-sen University (ethics number: SYXX2012-0081) and performed in accordance with the Guide to the Care and Use of Experimental Animals provided by the National Research Council (1996, USA).

### **Consent for publication**

Not applicable.

### **Availability of data and materials**

The analyzed data sets generated during the study are available from the corresponding author on reasonable request.

## Competing interests

The authors declare that they have no competing interests.

## Funding

This research was supported by the Medical Scientific Research Foundation of Guangdong Province of China (A2017207), which provided the location for experiments, animal feeding, fund for design of the study and collection, analysis, and interpretation of data.

## Author's contribution

LW designed and supervised the study. ZMP analyzed the data. TTL, XYZ and JD conduct the study and collected the data and written the manuscript. SBC, KZ collected and analyzed the data. YW, SYL edited the manuscript. All authors have read and approved the final manuscript.

## Acknowledgments

Not applicable.

## References

1. Dominguez, E., et al., *JAK/STAT3 pathway is activated in spinal cord microglia after peripheral nerve injury and contributes to neuropathic pain development in rat*. J Neurochem, 2008. **107**(1): p. 50-60.
2. Shibata, N., et al., *Activation of signal transducer and activator of transcription-3 in the spinal cord of sporadic amyotrophic lateral sclerosis patients*. Neurodegener Dis, 2009. **6**(3): p. 118-26.
3. LeComte, M.D., et al., *Notch1-STAT3-ETBR signaling axis controls reactive astrocyte proliferation after brain injury*. Proc Natl Acad Sci U S A, 2015. **112**(28): p. 8726-31.
4. Okada, S., et al., *Conditional ablation of Stat3 or Socs3 discloses a dual role for reactive astrocytes after spinal cord injury*. Nat Med, 2006. **12**(7): p. 829-34.
5. Tsuda, M., et al., *JAK-STAT3 pathway regulates spinal astrocyte proliferation and neuropathic pain maintenance in rats*. Brain, 2011. **134**(Pt 4): p. 1127-39.
6. Gu, F., et al., *Suppression of Stat3 promotes neurogenesis in cultured neural stem cells*. J Neurosci Res, 2005. **81**(2): p. 163-71.
7. Cao, F., et al., *Conditional deletion of Stat3 promotes neurogenesis and inhibits astrogliogenesis in neural stem cells*. Biochem Biophys Res Commun, 2010. **394**(3): p. 843-7.
8. Gong, Z., et al., *Stem cell transplantation: A promising therapy for spinal cord injury*. Curr Stem Cell Res Ther, 2019.
9. Assinck, P., et al., *Cell transplantation therapy for spinal cord injury*. Nat Neurosci, 2017. **20**(5): p. 637-647.



10. Muheremu, A., J. Peng, and Q. Ao, *Stem cell based therapies for spinal cord injury*. Tissue Cell, 2016. **48**(4): p. 328-33.
11. Lizee, G., et al., *Real-time quantitative reverse transcriptase-polymerase chain reaction as a method for determining lentiviral vector titers and measuring transgene expression*. Hum Gene Ther, 2003. **14**(6): p. 497-507.
12. Chen, N., et al., *Targeted Inhibition of Leucine-Rich Repeat and Immunoglobulin Domain-Containing Protein 1 in Transplanted Neural Stem Cells Promotes Neuronal Differentiation and Functional Recovery in Rats Subjected to Spinal Cord Injury*. Crit Care Med, 2016. **44**(3): p. e146-57.
13. Peng, Z., et al., *Inhibition of Notch1 signaling promotes neuronal differentiation and improves functional recovery in spinal cord injury through suppressing the activation of Ras homolog family member A*. J Neurochem, 2019. **150**(6): p. 709-722.
14. Basso, D.M., M.S. Beattie, and J.C. Bresnahan, *A sensitive and reliable locomotor rating scale for open field testing in rats*. J Neurotrauma, 1995. **12**(1): p. 1-21.
15. Zhao, X., et al., *Lentiviral vector delivery of short hairpin RNA to NgR1 promotes nerve regeneration and locomotor recovery in injured rat spinal cord*. Sci Rep, 2018. **8**(1): p. 5447.
16. Lee, D.Y., *Roles of mTOR Signaling in Brain Development*. Exp Neurobiol, 2015. **24**(3): p. 177-85.
17. Pfyffer, D., et al., *Tissue bridges predict recovery after traumatic and ischemic thoracic spinal cord injury*. Neurology, 2019. **93**(16): p. e1550-e1560.
18. Zhang, T., C. Liu, and L. Chi, *Suppression of miR-10a-5p in bone marrow mesenchymal stem cells enhances the therapeutic effect on spinal cord injury via BDNF*. Neurosci Lett, 2019: p. 134562.
19. Qian, D., et al., *Blocking Notch signal pathway suppresses the activation of neurotoxic A1 astrocytes after spinal cord injury*. Cell Cycle, 2019. **18**(21): p. 3010-3029.
20. Mothe, A.J. and C.H. Tator, *Review of transplantation of neural stem/progenitor cells for spinal cord injury*. Int J Dev Neurosci, 2013. **31**(7): p. 701-13.
21. Namiki, J. and C.H. Tator, *Cell proliferation and nestin expression in the ependyma of the adult rat spinal cord after injury*. J Neuropathol Exp Neurol, 1999. **58**(5): p. 489-98.
22. Herrmann, J.E., et al., *STAT3 is a critical regulator of astrogliosis and scar formation after spinal cord injury*. J Neurosci, 2008. **28**(28): p. 7231-43.
23. Kim, C., et al., *Mesenchymal Stem Cell Transplantation Promotes Functional Recovery through MMP2/STAT3 Related Astrogliosis after Spinal Cord Injury*. Int J Stem Cells, 2019. **12**(2): p. 331-339.
24. Cui, M., et al., *Effects of STAT3 inhibitors on neural functional recovery after spinal cord injury in rats*. Biosci Trends, 2017. **10**(6): p. 460-466.
25. Cheng, P.Y., et al., *Interplay between SIN3A and STAT3 mediates chromatin conformational changes and GFAP expression during cellular differentiation*. PLoS One, 2011. **6**(7): p. e22018.
26. Takizawa, T., et al., *DNA methylation is a critical cell-intrinsic determinant of astrocyte differentiation in the fetal brain*. Dev Cell, 2001. **1**(6): p. 749-58.

27. Natarajan, R., et al., *STAT3 modulation to enhance motor neuron differentiation in human neural stem cells*. PLoS One, 2014. **9**(6): p. e100405.
28. Russell, R.C., C. Fang, and K.L. Guan, *An emerging role for TOR signaling in mammalian tissue and stem cell physiology*. Development, 2011. **138**(16): p. 3343-56.
29. Lee, J.E., et al., *S6K Promotes Dopaminergic Neuronal Differentiation Through PI3K/Akt/mTOR-Dependent Signaling Pathways in Human Neural Stem Cells*. Mol Neurobiol, 2016. **53**(6): p. 3771-3782.
30. van Gorp, S., et al., *Amelioration of motor/sensory dysfunction and spasticity in a rat model of acute lumbar spinal cord injury by human neural stem cell transplantation*. Stem Cell Res Ther, 2013. **4**(3): p. 57.
31. Winkler, T., et al., *Topical application of dynorphin A (1-17) antiserum attenuates trauma induced alterations in spinal cord evoked potentials, microvascular permeability disturbances, edema formation and cell injury: an experimental study in the rat using electrophysiological and morphological approaches*. Amino Acids, 2002. **23**(1-3): p. 273-81.
32. Ramadan, W.S., et al., *Histological, immunohistochemical and ultrastructural study of secondary compressed spinal cord injury in a rat model*. Folia Histochem Cytobiol, 2017. **55**(1): p. 11-20.
33. Hosseini, S.M., et al., *Concomitant use of mesenchymal stem cells and neural stem cells for treatment of spinal cord injury: A combo cell therapy approach*. Neurosci Lett, 2018. **668**: p. 138-146.
34. Lopez-Serrano, C., et al., *Effects of the Post-Spinal Cord Injury Microenvironment on the Differentiation Capacity of Human Neural Stem Cells Derived from Induced Pluripotent Stem Cells*. Cell Transplant, 2016. **25**(10): p. 1833-1852.
35. Squair, J.W., et al., *High Thoracic Contusion Model for the Investigation of Cardiovascular Function after Spinal Cord Injury*. J Neurotrauma, 2017. **34**(3): p. 671-684.

## Figures

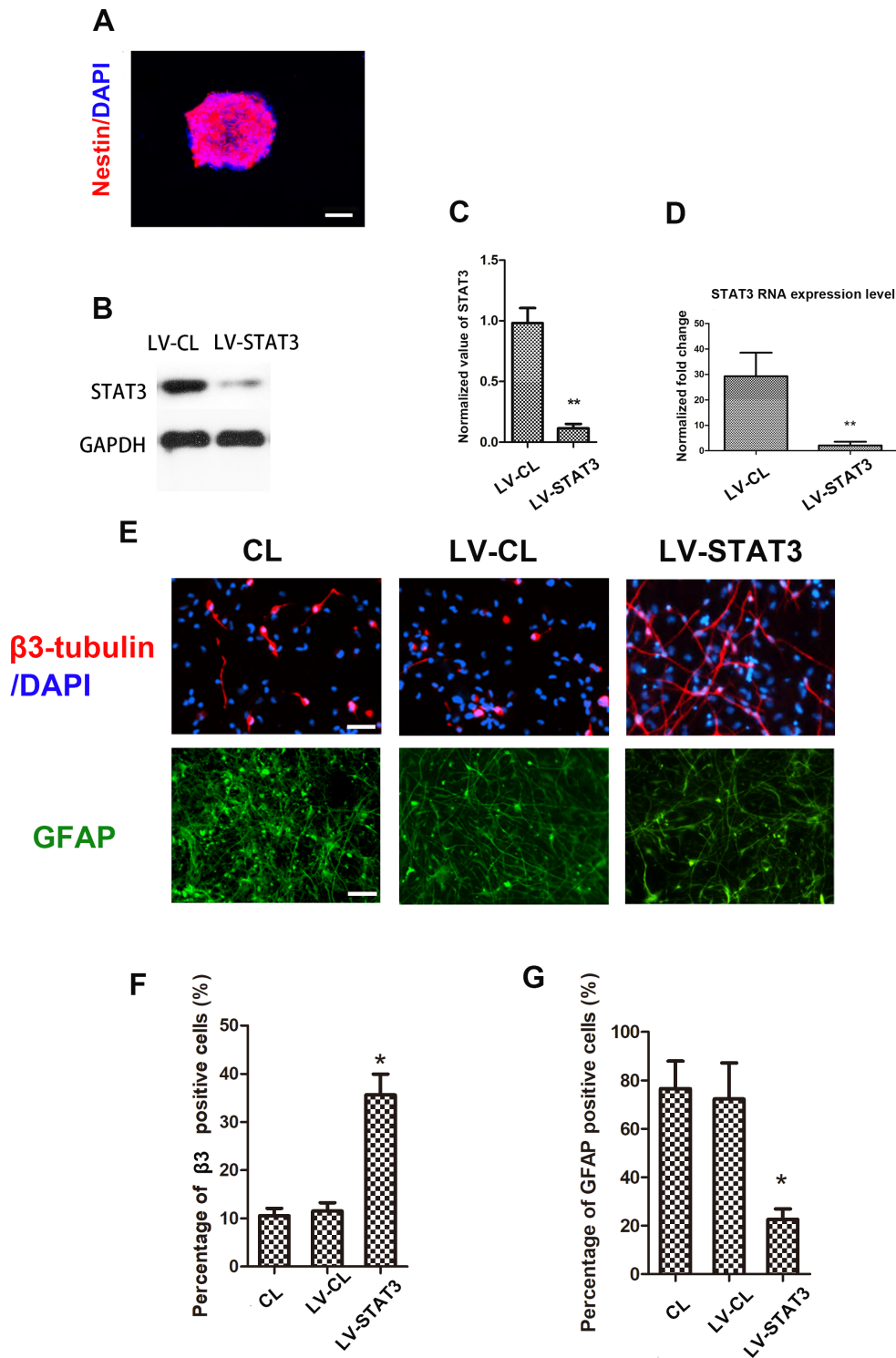


**Figure 1**

Knockdown of STAT3 promoted neuronal differentiation in NSCs (A) Immunofluorescence indicated that the NSC-specific marker nestin was highly expressed in cells. (B) Western blot was used to measure STAT3 protein levels in each group. (C) Quantification of Western blot for STAT3 expression (compared with GAPDH). (D) Effect of STAT3 gene silencing on RNA expression by quantitative RT-PCR (compared with GAPDH). (E) Immunostaining for  $\beta$ 3-tubulin (red), GFP (green) and DAPI (blue) in each group. (F, G)

Quantification of the percentage of  $\beta$ 3-tubulin- and GFAP-positive cells in each group. Scale bar=50  $\mu$ m, \*P<0.05, \*\*P<0.01.

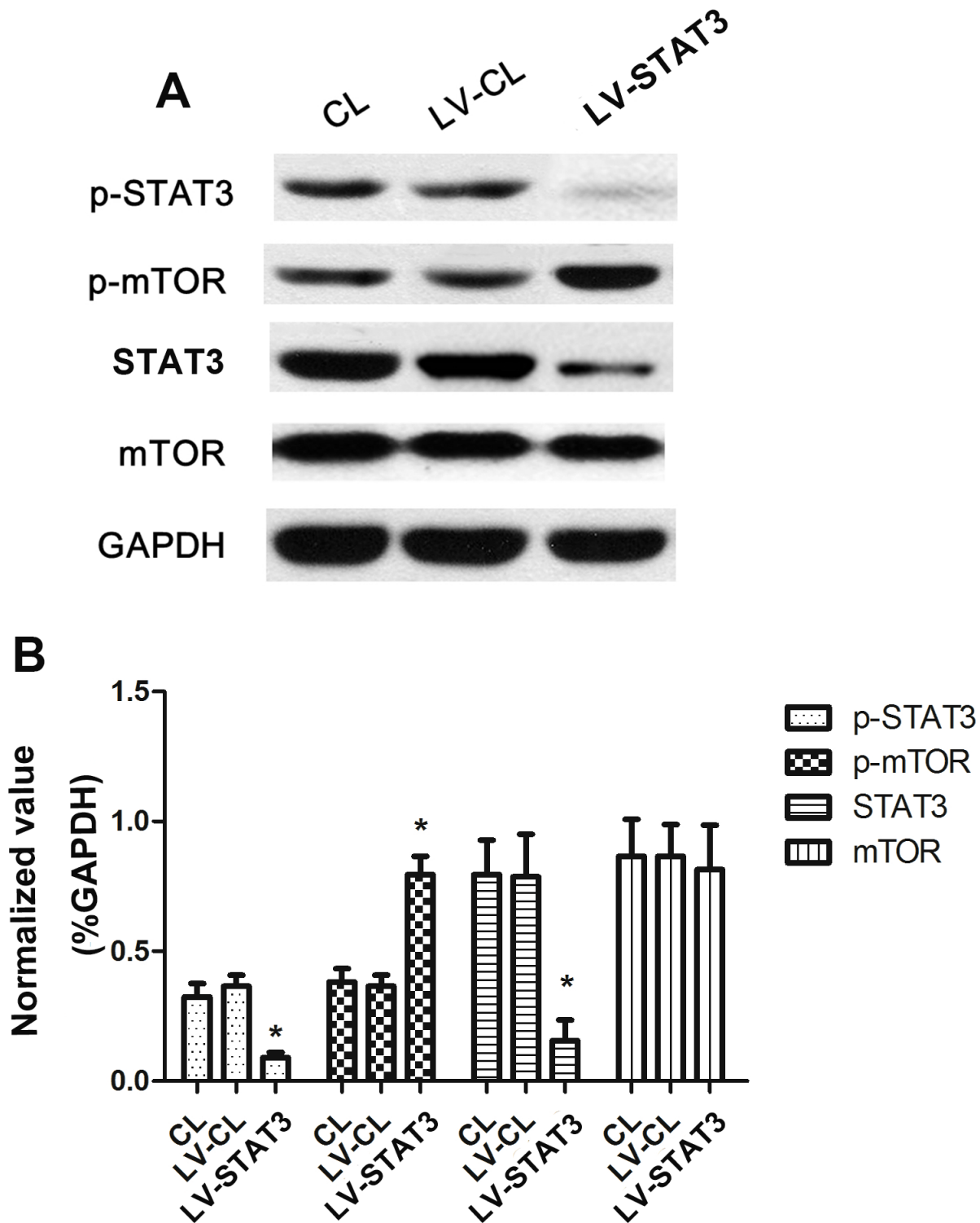
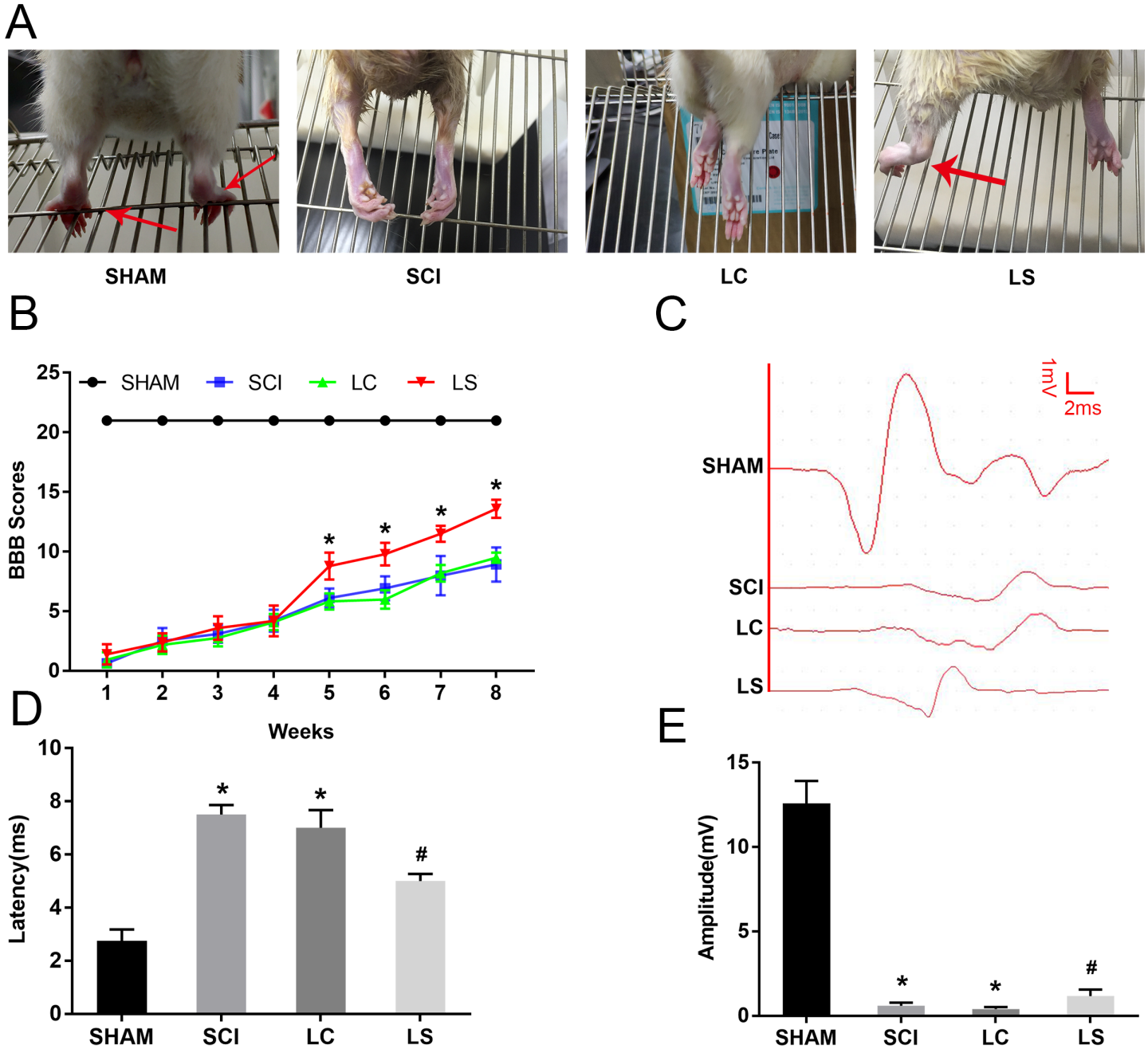


Figure 2

Targeted inhibition of STAT3 promoted mTOR activation. (A) Western blotting analysis of STAT3, mTOR, p-STAT3, p-mTOR and glyceraldehyde 3-phosphate dehydrogenase (GAPDH) expression in each group.

(B) Quantification of Western blot for STAT3, mTOR, p-STAT3, and p-mTOR expression. \* $P < 0.05$ , \*\* $P < 0.01$ .



**Figure 3**

Transplantation of STAT3-RNAi-treated NSCs enhanced functional recovery after SCI. (A) Images showing hindlimb movements in the sham, SCI, LC, and LS groups. Red arrows indicate weight-supported stepping. (B) BBB scores in different groups. (C) Electrophysiologic outcomes of SCEP recordings. (D, E) Quantification of the latency and amplitude of the SCEP. \* $P < 0.05$ , vs sham, #  $P < 0.05$ , vs LC. SHAM: rats without transection of the spinal cord group; SCI: rats with complete transection of the spinal cord; LC: LV-control shRNA-transfected NSCs were injected into rats with SCI; LS: LV-STAT3 shRNA-transfected NSCs were injected into rats with SCI.

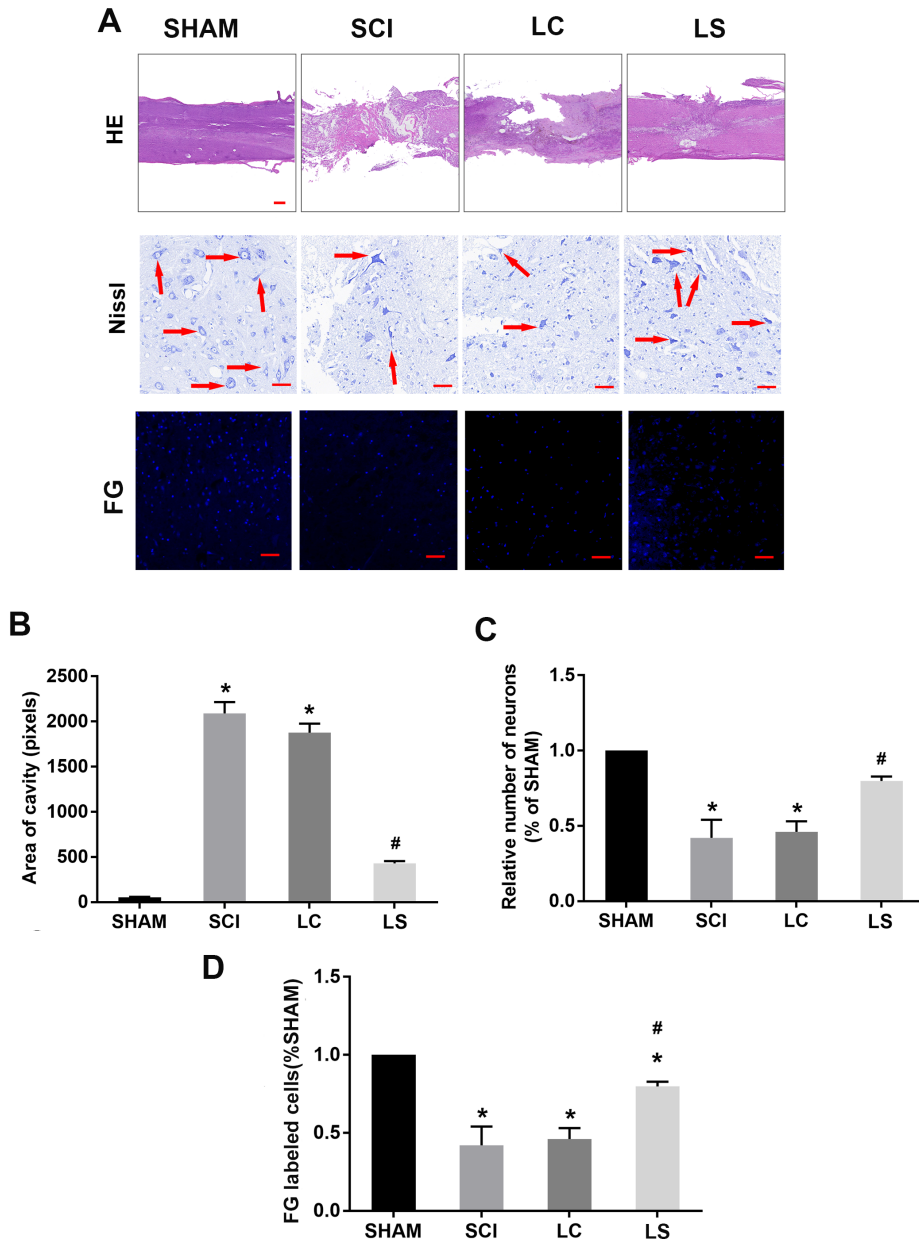


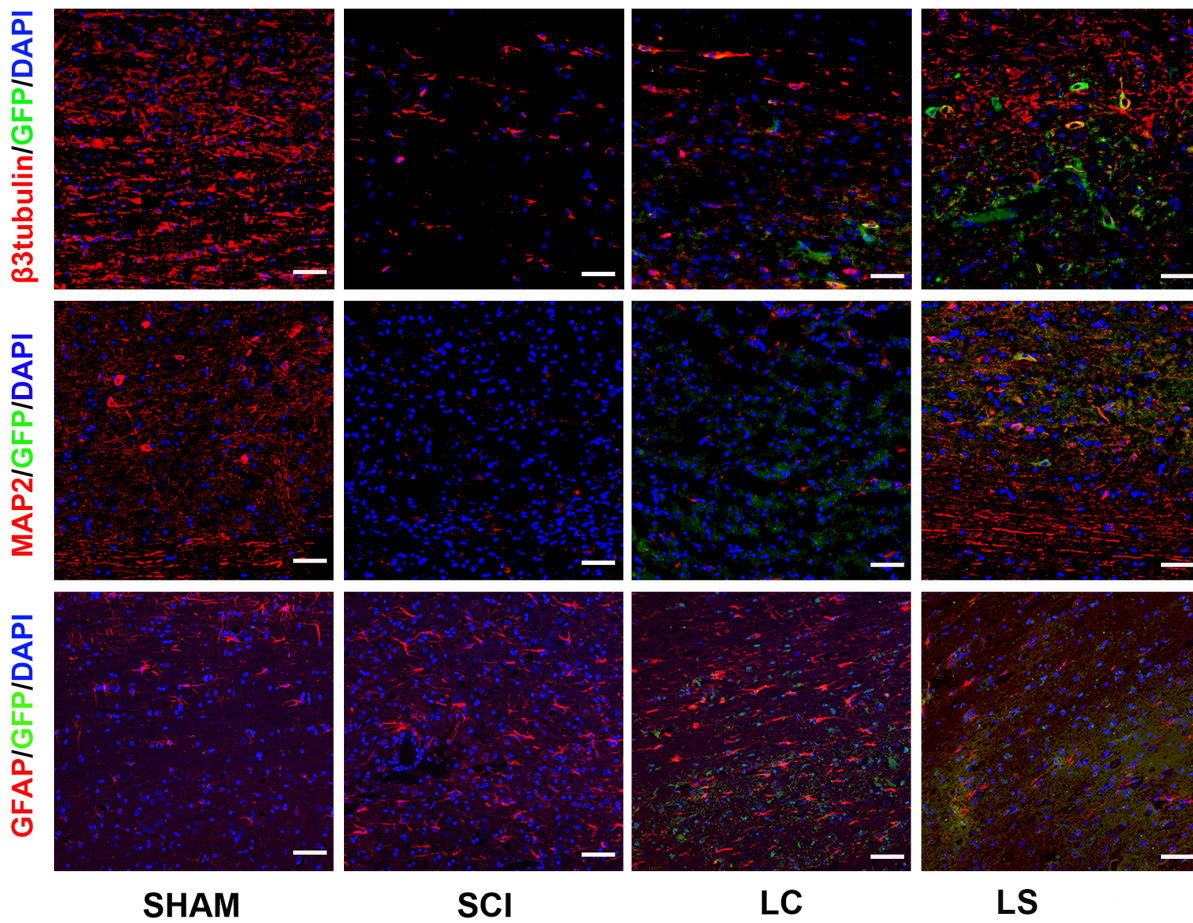
**Figure 4**

Transplantation of STAT3-RNAi-treated NSCs enhanced tissue repair after SCI. (A) Representative H&E staining micrographs showing cavity formation in the sham, SCI, LC, and LS groups (N=6) at the eighth week post injury. Images of surviving neurons at 3 mm rostral to the injured epicenter by Nissl staining. Red arrows point to surviving neurons. Immunofluorescence showing FG-labeled neurons in the ventricolumna of the T8 segment spinal cord. (B) Comparison of the cavity area in each group. (C)



Relative number of FG-labeled neurons in each group. (D) Quantification analysis of the number of FG-labeled cells in each group (compared with that in the sham group). \* P < 0.05, vs sham, #P < 0.05, vs LC. Scale bar= 100µm.

**A**



**B**

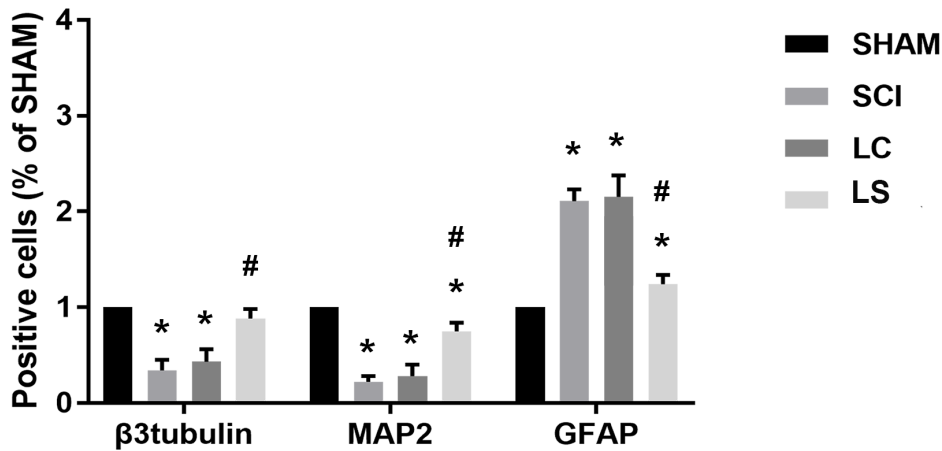


**Figure 5**

Targeted inhibition of STAT3 enhanced neuronal differentiation of transplanted NSCs in the spinal cord lesions. (A) Immunostaining for β3-tubulin, MAP2, GFAP, GFP and DAPI showing the differentiation of the

transplanted NSCs in the spinal cord lesions in each group. (B) Quantification analysis of the number of  $\beta$ 3-tubulin-, MAP2- and GFAP-positive cells in each group (compared with that in the sham group). \*  $P < 0.05$ , vs sham, #  $P < 0.05$ , vs LC. Scale bar= 100 $\mu$ m.

## Supplementary Files

This is a list of supplementary files associated with this preprint. Click to download.

- [NC3RsARRIVEGuidelinesChecklist2014.docx](#)